Journal of the European Ceramic Society 21 (2001) 2109–2112

www.elsevier.com/locate/jeurceramsoc

Effects of Li and Mg doping on microstructure and properties of sol-gel ZnO thin films

Shinobu Fujihara *, Chikako Sasaki, Toshio Kimura

Department of Applied Chemistry, Faculty of Science and Technology, Keio University, 3-14-1, Hiyoshi, Kohoku-ku, Yokohama 223-8522, Japan

Received 4 September 2000; received in revised form 23 October 2000; accepted 30 October 2000

Abstract

Zinc oxide thin films doped with Li and Mg were prepared by the sol-gel method, and effects of doping on microstructure and electrical properties were examined. The doped films exhibited *c*-axis-orientation after final heating at 500°C for 30 min in flowing oxygen. The ZnO crystallite size increased by doping and the surface of the films became rougher. The current density of the films was reduced by doping probably due to the formation of acceptor levels (Li-doping) and the reduction of oxygen defects (Mg-doping). The film with a nominal composition of $Zn_{0.85}Li_{0.10}Mg_{0.05}O$ showed the lowest current density of 1.7×10^{-6} A cm^{-2} in the present study.

Keywords: Electrical properties; Films; Grain growth; Sol–gel processes; ZnO

1. Introduction

Zinc oxide (ZnO) is an *n*-type semiconductor with a band-gap of 3.2 eV.[1] Recently, a ferroelectric phase transition at temperatures 330–470 K was found in Li-doped ZnO ceramic specimens.[2–4] The spontaneous polarization of $Zn_{0.9}Li_{0.1}O$ was 0.9 μC cm^{-2} along the *c*-axis at room temperature. Joseph et al.[5] prepared ZnO:Li films by pulsed laser deposition and observed ferroelectric behavior. It is known that ZnO exhibits a wide range of the resistivity from 10^{-4} to 10^{10} Ωcm.[6,7] In the case of ferroelectric device application, the leakage current density should be as low as 10^{-6} A cm^{-2}.[8,9] Reduction of carriers, suppression of oxygen defects and control of the microstructure are supposed to be crucial to reach this value.

A number of different techniques have been utilized to prepare ZnO thin films. The sol-gel method is one of the attractive processes due to controllability of compositions, simple facilities, low cost, etc. The films with preferential *c*-axis-orientation of ZnO grains perpendicular to the substrate can be easily obtained by the sol-gel process.[10] In the present work, we investigated effects of Li and Mg doping on the microstructure and properties of ZnO films.

2. Experimental procedure

$Zn(CH_3COO)_2\cdot2H_2O$ and LiCl or $MgCl_2\cdot6H_2O$ were dissolved in 2-methoxyethanol, and monoethanolamine was added to the solution. The concentration of metal ions was 0.75 mol/l and nominally x and y values in "$Zn_{1-x-y}Li_xMg_yO$" were varied from 0 to 0.20 (for x) or 0.10 (for y). The solution was stirred at 60°C for 1 h with reflux, and then dip-coated on Pyrex glass substrates. The coating films were dried at 300°C for 2 min immediately after coating. After repeating the coating procedure five times, the films were finally heated at 500°C for 30 min in flowing oxygen. The films are distinguished with their nominal compositions using x and y values hereafter, since quantitative analysis of dopants has not been done.

The crystalline structure of the films was confirmed by X-ray diffraction (XRD) analysis using CuK_α radiation with a Jeol JDX-8P diffractometer. The crystallite size of ZnO was determined using the Scherrer's equation, $D=0.9\lambda/(\beta\cos\theta)$, where D is the crystal size, λ the X-ray wavelength, β the broadening of the diffraction peak and θ the diffraction angle. X-ray photoelectron spectroscopy (XPS) was carried out using MgK_α radiation with a Jeol JSP-9000MX. The microstructure was observed by field emission scanning electron microscopy (FESEM) with a Hitachi S-4700 microscope. The current density of the films was measured by a two probe method with Au electrodes.[11]

* Corresponding author. Tel.: +81-45-566-1581; fax: +81-45-566-1551.

E-mail address: shinobu@applc.keio.ac.jp (S. Fujihara).

0955-2219/01/$ - see front matter
PII: S0955-2219(01)00182-0

3. Results and discussion

Fig. 1 shows XRD patterns of the Li-doped ZnO films after the final heat treatment at 500°C. Any of the films exhibits a strong (002) peak, indicating the *c*-axis orientation of ZnO grains perpendicular to the substrate. It is also seen that the intensity of the (002) peak increases with Li-doping up to $x = 0.15$. The ZnO crystallite size is summarized in Table 1. Non-doped ZnO has the size of 19.6 nm, while the Li-doped ZnO has slightly larger sizes with typical 27.0 nm for $x = 0.05$. It is believed that the interstitial zinc plays an important role in the grain growth of ZnO.[1,12] In the case of trivalent Al-doping, the concentration of the zinc interstitials is reduced, resulting in the suppressed grain growth of ZnO. This is because the diffusivity is decreased in ZnO. A similar effect can be observed in F-doped ZnO.[13] On the contrary, Li-doping mainly occurs as follows,[1]

$$Li_2O \rightarrow Li'_{Zn} + Li_i^+ + O_O,$$

where Li'_{Zn} represents lithium on zinc lattice site, Li_i^+ lithium in interstitial position, and O_O oxygen on lattice site. Since Li^+ has a smaller ionic radius of 0.060 nm than Zn^{2+} having 0.074 nm, the diffusivity in the Li-doped ZnO is expected to be higher. The present results coincide with this consideration.

Fig. 2 shows FESEM photographs of the surface of the films. The increase in the grain size by Li-doping can be observed. Uniform size distribution is also seen. However, the Li-doped film becomes porous as compared to the non-doped ZnO film. Although we have been trying to optimize the drying and heating process, the condition employed is not suitable for the densification of the films at present. The thickness of the films was on the order of 200 nm according to the cross-sectional observation.

The Au electrode has higher work function than ZnO and the Au/ZnO contact forms Schottky barrier.[14,15]

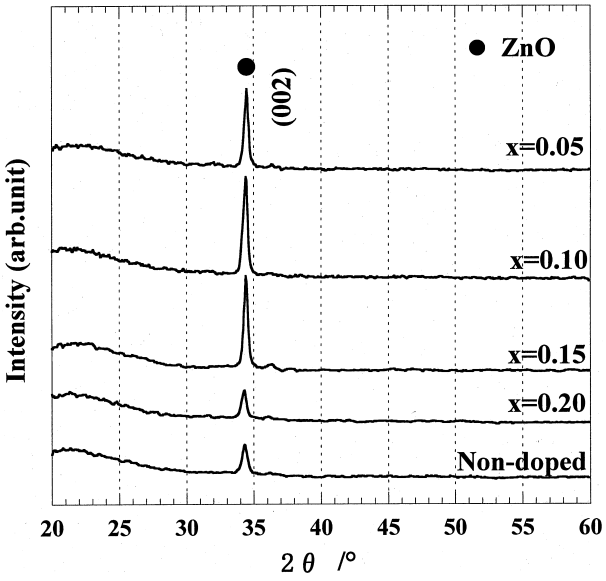

Fig. 1. XRD patterns of the non-doped and Li-doped ZnO (nominal $Zn_{1-x}Li_xO$) thin films after heating at 500°C for 30 min.

Table 1
The crystallite size, the current density at 5 V, and the ρ/ρ_0 values of the Li- and Mg-doped ZnO thin films with nominal compositions of $Zn_{1-x-y}Li_xMg_yO$

Dopant	Nominal composition	Crystallite size (nm)	Current density (A cm^{-2})	ρ/ρ_0
	ZnO	19.6	1.9×10^{-4}	1
Li	$x=0.05$	27.0	4.6×10^{-5}	4.2
	$x=0.10$	25.1	3.0×10^{-6}	65.4
	$x=0.15$	22.4	5.5×10^{-6}	34.6
	$x=0.20$	20.0	1.5×10^{-5}	13.1
Mg	$y=0.01$	24.0	1.2×10^{-4}	1.6
	$y=0.03$	26.4	1.5×10^{-5}	13.1
	$y=0.05$	24.9	1.0×10^{-5}	19.2
	$y=0.10$	30.6	–	–
Li, Mg	$x=0.10$, $y=0.03$	22.2	3.2×10^{-6}	61.5
	$x=0.10$, $y=0.05$	24.8	1.7×10^{-6}	115.4
	$x=0.15$, $y=0.05$	25.1	4.4×10^{-6}	42.3

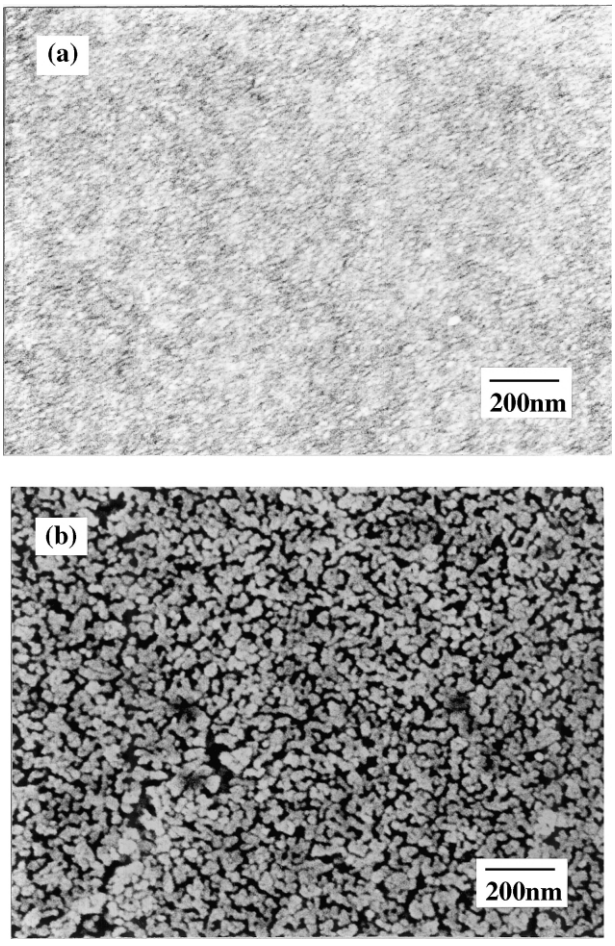

Fig. 2. FESEM photographs of the surface of the (a) non-doped and (b) Li-doped ($x = 0.10$) ZnO thin films.

Therefore, the current (I)–voltage (V) characteristic of the Au/ZnO(:Li)/Au structure is nonlinear. Nevertheless, Li-doping obviously reduces the current density of the films as shown in Fig. 3. Doping of 10 mol% Li is optimal. At an applied voltage of 5 V, the current density is in the order of 3.0×10^{-6} A cm^{-2} as summarized in Table 1. The reduced current density is attributed to the replacement reaction of the Li interstitials as follows,[1,16]

$$Li_i^+ + Zn_{Zn} + e^- \rightarrow Li'_{Zn} + Zn_i^+$$

or

$$Li_i^+ + e^- \rightarrow Li'_{Zn} + V_O^+$$

For $x=0.15$ and 0.20, the current density is higher than that for $x=0.10$. A similar result was reported previously for the spray pyrolysed ZnO films.[17] With the fact that the grain size is smaller in these two films as read from Table 1, we can assume that too much lithium is not soluble in ZnO lattice and segregates probably in the grain boundary.

ZnO exhibited *c*-axis orientation with Mg-doping up to $y=0.05$ as confirmed by XRD. (100) and (101) peaks also appeared in the film with $y=0.10$. No peaks due to rock-salt MgO were observed in any film. The film of $y=0.10$ was often exfoliated off the substrate after the heat treatment. The Scherrer crystallite size increased by Mg-doping as shown in Table 1. Although the role of isovalent Mg^{2+} is not clear, a smaller ionic radius of 0.065 nm may be effective for diffusivity. The XPS analysis of Mg revealed that Mg was bonded with oxygen and peak intensity of Mg 2p increased with increasing *y* value.

Fig. 4 shows FESEM photograph of the surface of the film with $y=0.05$. The surface is rougher and the grain size is larger compared to the Li-doped film shown in Fig. 2.

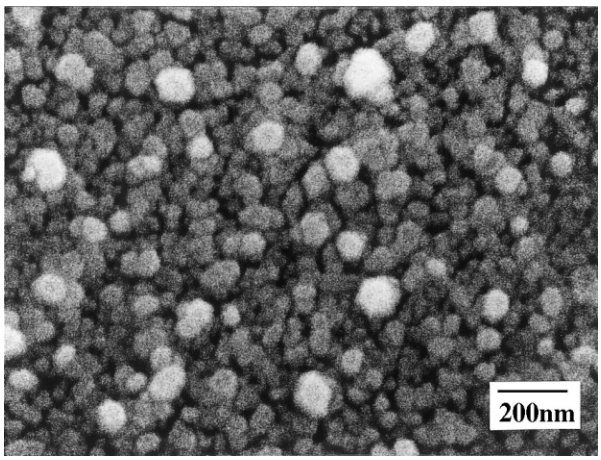

Fig. 4. FESEM photographs of the surface of the Mg-doped ($y=0.05$) ZnO thin film.

Fig. 5 shows I–V characteristics of the films. The current density decreases with increasing *y* value. At the applied voltage of 5 V, the current density of 1.0×10^{-5} A cm^{-2} is obtained for $y=0.05$, which is larger than that of the Li-doped ZnO with $x=0.10$. Substitution of Mg^{2+} for Zn^{2+} has no significant contribution to the cation charge in ZnO. In spite of this, the current density was reduced. The *n*-type conduction of ZnO is attributed to the interstitial zinc and/or oxygen vacancy. Therefore, the above result should be explained by the decrease of the oxygen defects by Mg-doping since Mg–O bond has more ionic character than Zn–O.[3]

A ZnO thin film co-doped with Li and Mg (nominal $Zn_{0.85}Li_{0.10}Mg_{0.05}O$) was prepared on the basis of the above results. The film was also *c*-axis oriented. The Scherrer crystallite size was calculated to be 24.8 nm, which was larger than that of the non-doped ZnO. The

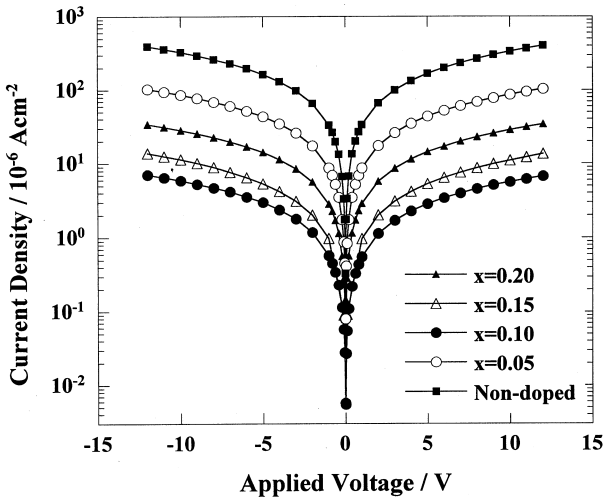

Fig. 3. I–V characteristic of the Li-doped ZnO thin films.

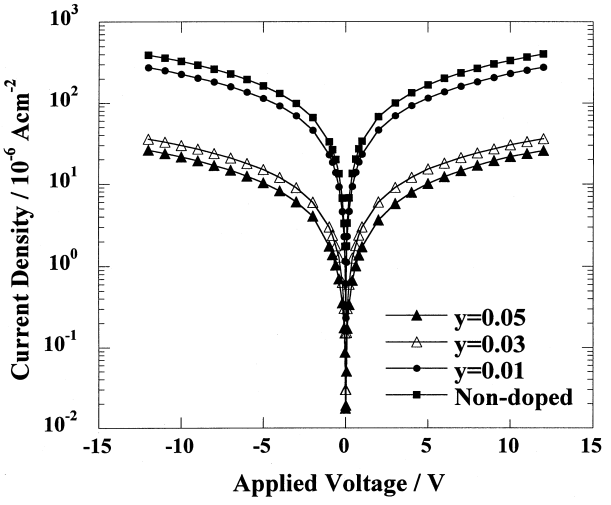

Fig. 5. I–V characteristic of the Mg-doped ZnO thin films.

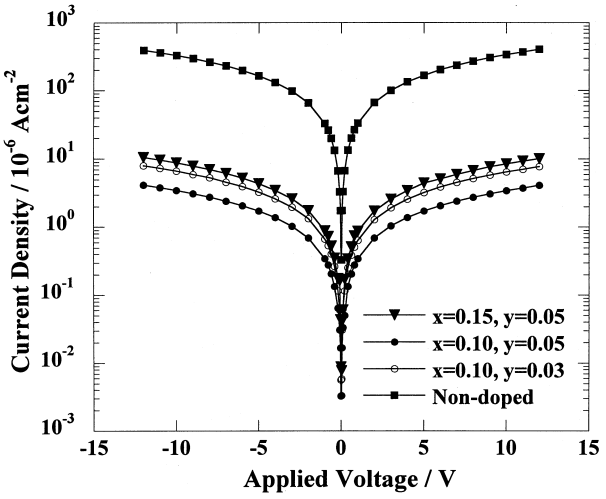

Fig. 6. I–V characteristic of the ZnO thin films co-doped with Li and Mg.

SEM observation revealed that the surface of the film was composed of grains with the size of 40–60 nm. No remarkable change in the microstructure was observed between the Li-doped and the Li,Mg-doped ZnO films.

Fig. 6 shows I–V characteristics of the film. The current density is lowest among all the films prepared in the present study. The value at the applied voltage of 5 V is 1.7×10^{-6} A cm^{-2}. This can be explained by mixed effects of Li-doping with the formation of the acceptor level and Mg-doping with the reduction of the oxygen defects. Other compositions, nominal $Zn_{0.87}Li_{0.10}Mg_{0.03}O$ and $Zn_{0.80}Li_{0.15}Mg_{0.05}O$, were also examined, which resulted in an increased current density.

Finally we estimated a ratio ρ/ρ_0 from the I–V measurement of the films where ρ and ρ_0 are the electrical resistivity of the doped and non-doped ZnO films as listed in the last column of Table 1. The resistivity of the doped ZnO films is predominantly determined by the film compositions. Keeping the resistivity high, the microstructure of the films should be improved in further work.

References

1. Bonasewicz, P., Hirschwald, W. and Neumann, G., Influence of surface processes on electrical, photochemical, and thermodynamical properties of zinc oxide films. *J. Electrochem. Soc.*, 1986, **133**, 2270–2278.
2. Onodera, A., Tamaki, N., Kawamura, Y., Sawada, T. and Yamashita, H., Dielectric activity and ferroelectricity in piezoelectric semiconductor Li-doped ZnO. *Jpn. J. Appl. Phys.*, 1996, **35**, 5160–5162.
3. Onodera, A., Tamaki, N., Jin, K. and Yamashita, H., Ferroelectric properties in piezoelectric semiconductor $Zn_{1-x}M_xO$ (M = Li, Mg). *Jpn. J. Appl. Phys.*, 1997, **36**, 6008–6011.
4. Onodera, A., Tamaki, N., Yoshio, K., Satoh, H., Takama, T. and Yamashita, H., Novel ferroelectricity in polar semiconductor ZnO by Li-substitution. In *Proceedings of the Eleventh IEEE International Symposium on Applications of Ferroelectrics*, ed. E. Colla, D. Damjanovic and N. Setter. The Institute of Electrical and Electronic Engineers, NJ, 1998, pp. 475–478.
5. Joseph, M., Tabata, H. and Kawai, T., Ferroelectric behavior of Li-doped ZnO thin films on Si(100) by pulsed laser deposition. *Appl. Phys. Lett.*, 1999, **74**, 2534–2536.
6. Korb, E. D. and Laudise, R. A., Hydrothermally grown ZnO crystals of low and intermediate resistivity. *J. Am. Ceram. Soc.*, 1966, **49**, 302–305.
7. Hu, J. and Gordon, R. G., Textured aluminium-doped zinc oxide thin films from atmospheric pressure chemical-vapor deposition. *J. Appl. Phys.*, 1992, **71**, 880–890.
8. Hu, H. and Krupanidhi, S. B., Current–voltage characteristics of ultrafine-grained ferroelectric $Pb(Zr,Ti)O_3$ thin-films. *J. Mater. Res.*, 1994, **9**, 1484–1498.
9. Bhattacharya, P., Park, K. and Nishioka, Y., Comparative study of amorphous and crystalline $(Ba,Sr)TiO_3$ thin-films deposited by laser-ablation. *Jpn. J. Appl. Phys.*, 1994, **33**, 4103–4106.
10. Ohyama, M., Kozuka, H., Yoko, T. and Sakka, S., Preparation of ZnO thin films with preferential orientation by sol-gel method. *J. Ceram. Soc. Jpn.*, 1996, **104**, 296–300.
11. Fujihara, S., Sasaki, C. and Kimura, T., Preparation of Al- and Li-doped ZnO thin films by sol-gel method. *Key Eng. Mater.*, 2000, **181–182**, 109–112.
12. Ohya, Y., Saiki, H., Tanaka, T. and Takahashi, Y., Microstructure of TiO_2 and ZnO films fabricated by the sol-gel method. *J. Am. Ceram. Soc.*, 1996, **79**, 825–830.
13. Fujihara, S., Kusakado, J. and Kimura, T., Fluorine doping in transparent conductive ZnO thin films by a sol-gel method using trifluoroacetic acid. *J. Mater. Sci. Lett.*, 1998, **17**, 781–783.
14. Sundaram, K. B. and Khan, A., Work function determination of zinc oxide films. *J. Vac. Sci. Technol. A*, 1997, **15**, 428–430.
15. Traversa, E. and Bearzotti, A., Humidity sensitive electrical properties of dense ZnO with non-ohmic electrode. *J. Ceram. Soc. Jpn.*, 1995, **103**, 11–15.
16. Srivastava, J. K., Agarwal, L. and Bhattacharyya, A. B., Electrical characteristics of lithium-doped ZnO films. *J. Electrochem. Soc.*, 1989, **136**, 3414–3417.
17. Pushparajah, P., Arof, A. K. and Radhakrishna, S., Physical properties of spray pyrolysed pure and doped ZnO thin films. *J. Phys. D*, 1994, **27**, 1518–1521.